

$\Omega_c \rightarrow \pi^+(\pi^0, \eta)\pi\Xi^*$, $\pi^+(\pi^0, \eta)\bar{K}\Sigma^*$ reactions and the two $\Xi(1820)$ statesWei-Hong Liang,^{1,2,3,*} Raquel Molina,^{2,†} and Eulogio Oset^{1,2,‡}¹*Department of Physics, Guangxi Normal University, Guilin 541004, China*²*Departamento de Física Teórica and IFIC, Centro Mixto Universidad de Valencia-CSIC, Institutos de Investigación de Paterna, Apartado 22085, 46071 Valencia, Spain*³*Guangxi Key Laboratory of Nuclear Physics and Technology, Guangxi Normal University, Guilin 541004, China*

(Received 14 May 2024; accepted 11 July 2024; published 7 August 2024)

We have studied the $\Omega_c \rightarrow \pi^+(\pi^0, \eta)\pi\Xi^*$ and $\Omega_c \rightarrow \pi^+(\pi^0, \eta)\bar{K}\Sigma^*$ decays, where the final $\pi\Xi^*$ or $\bar{K}\Sigma^*$ comes from the decay of two resonances around the nominal $\Xi(1820)$, which are generated from the interaction of coupled channels made of a pseudoscalar and a baryon of the decuplet. The $\pi\Xi^*$ mass distributions obtained in the six different reactions studied are quite different, and we single out four of them, which are free of a tree level contribution, showing more clearly the effect of the resonances. The lower mass resonance is clearly seen as a sharp peak, but the higher mass resonance manifests itself through an interference with the lower one that leads to a dip in the mass distribution around 1850 MeV. Such a feature is similar to the dip observed in the S -wave $\pi\pi$ cross section around the 980 MeV coming from the interference of the $f_0(500)$ and $f_0(980)$ resonances. Its observation in coming upgrades of present facilities will shed light on the existence of these two resonances and their nature. On the other hand, when the $\Omega_c \rightarrow \pi^+(\pi^0, \eta)\bar{K}\Sigma^*$ reactions are studied, both peaks are observed.

DOI: 10.1103/PhysRevD.110.036005

I. INTRODUCTION

The issue of hadronic resonances corresponding to two nearby states with the same quantum numbers has been present for some time, since the challenging claim in Refs. [1,2] that the $\Lambda(1405)$ corresponded actually to two physical states. In technical words, this means two nearby poles in the same Riemann sheet, not the shadow poles encountered in different Riemann sheets corresponding to the same physical state. This issue was controversial at that time, but evidence from many theoretical calculations and different experiments opened the doors of the PDG [3] to the existence of two $\Lambda(1405)$ states, and in the 2020 edition of the PDG [4] two $\Lambda(1405)$ states were officially admitted (see review paper on this issue [5] on the PDG [3]).

The case of the two $\Lambda(1405)$ states opened the gates to the appearance of many other similar cases, one of them the two $K_1(1270)$ axial vector resonances, which were found in Ref. [6], and were supported experimentally as discussed in

Ref. [7]. New cases were found for two $D_0^*(2400)$ [now $D_0^*(2300)$] states in Refs. [8,9], and, in the study of the $3/2^-$ baryons coming from the interaction of pseudoscalar mesons with baryons of the $3/2^+$ decuplet [10,11], two states also emerged for the $\Xi(1820)$ resonance [11]. There are also cases found from experimental analyses, as the splitting of the $Y(4240)$ resonance reported by BABAR [12,13] into two states $Y(4230)$ and $Y(4260)$, suggested by the BESIII Collaboration [14]. In a recent paper [15] the authors show that the use of the Weinberg-Tomozawa interaction as the leading term of the chiral potentials gives rise to a double pole structure of some states. A global view on the issue of the double poles in hadronic resonances is presented in Ref. [16].

Recently the BESIII Collaboration reported on the reaction $\psi(3686) \rightarrow \bar{\Xi}^+ K^- \Lambda$ [17], where an inspection of the $K^- \Lambda$ mass distribution showed two distinct peaks, one corresponding to the $\Xi(1690)$ resonance and another one associated with the $\Xi(1820)$, yet with a width (~ 73 MeV) about 3 times bigger than the average width reported by the PDG [3] (~ 24 MeV). This apparent contradiction prompted a theoretical work [18], where it was found that the apparent large width was a consequence of the contribution of the two $\Xi(1820)$ resonances. Updating the work of Ref. [11], two poles were found in Ref. [18], one at 1824 MeV with a width of 62 MeV, and a second one at 1875 MeV with a large width of 260 MeV, and, with the contribution of the

*Contact author: liangwh@gxnu.edu.cn

†Contact author: raquel.molina@ific.uv.es

‡Contact author: Oset@ific.uv.es

two states, a good reproduction of the BESIII mass distribution could be achieved.

In the present work, we look for alternative reactions that can give information on the two $\Xi(1820)$ states. The reactions are based on the weak decay of the Ω_c^0 state and several decay channels are considered. On the one hand, we have

$$\begin{aligned}\Omega_c^0 &\rightarrow \pi^+\Xi(1820) \rightarrow \pi^+\pi^0\Xi^{*-}(\pi^-\Xi^{*0}), \\ \Omega_c^0 &\rightarrow \pi^0\Xi(1820) \rightarrow \pi^0\pi^+\Xi^{*-}(\pi^0\Xi^{*0}), \\ \Omega_c^0 &\rightarrow \eta\Xi(1820) \rightarrow \eta\pi^+\Xi^{*-}(\pi^0\Xi^{*0}).\end{aligned}\quad (1)$$

On the other hand, we have

$$\begin{aligned}\Omega_c^0 &\rightarrow \pi^+\Xi(1820) \rightarrow \pi^+\bar{K}^0\Sigma^{*-}(K^-\Sigma^{*0}), \\ \Omega_c^0 &\rightarrow \pi^0\Xi(1820) \rightarrow \pi^0\bar{K}^0\Sigma^{*0}(K^-\Sigma^{*+}), \\ \Omega_c^0 &\rightarrow \eta\Xi(1820) \rightarrow \eta\bar{K}^0\Sigma^{*0}(K^-\Sigma^{*+}).\end{aligned}\quad (2)$$

In the case of Eq. (1), we find a clear contribution of the two states in all these reactions, but showing in a peculiar way, through a destructive interference that leads to a pronounced dip in the $\pi\Xi^*$ mass distribution around 1850 MeV. This situation reminds one of the same features seen in the $\pi\pi$ isospin $I = 0$, S -wave scattering, where the cross section has a broad peak corresponding to the $f_0(500)$ resonance and a dip corresponding to the $f_0(980)$ [19,20] (see also this dip in the $0^{++}\pi^0\pi^0$ mode in J/ψ radiative decay to two pions [21]).

We shall also see different shapes of the mass distributions for these reactions reflecting the presence of more than one resonance. This was one of the experimental arguments used in favor of the two $\Lambda(1405)$ states by comparing the different shapes of the $\pi\Sigma$ mass distribution in the $\pi^-p \rightarrow K^0\pi\Sigma$ [22] and $K^-p \rightarrow \pi^0\pi^0\Sigma^0$ [23] (see the discussion on this issue in Ref. [24]). On the other hand, we will see that, in the reactions of $\Omega_c^0 \rightarrow \pi^+(\pi^0, \eta)\bar{K}\Sigma^*$ both peaks are observed.

II. FORMALISM

A. The two $\Xi^*(1820)$ states

In Ref. [11], the coupled channels of pseudoscalar meson-baryon ($3/2^+$) leading to baryons with strangeness $S = -2$ were considered, and with the interaction borrowed from chiral Lagrangians and a unitary scheme, two Ξ^* states with $3/2^-$ emerged. An update of the approach is done in Ref. [18] and the amplitudes obtained there are used here. The coupled channels are

$$\bar{K}^0\Sigma^{*-}, \quad K^-\Sigma^{*0}, \quad \pi^0\Xi^{*-}, \quad \eta\Xi^{*-}, \quad \pi^-\Xi^{*0}, \quad K^0\Omega^-, \quad (3)$$

with charge $Q = -1$, and

$$\bar{K}^0\Sigma^{*0}, \quad K^-\Sigma^{*+}, \quad \pi^+\Xi^{*-}, \quad \pi^0\Xi^{*0}, \quad \eta\Xi^{*0}, \quad K^+\Omega^-, \quad (4)$$

with charge $Q = 0$. The interaction (potential) is given by

$$V_{ij} = -\frac{1}{4f^2}C_{ij}(k^0 + k'^0); \quad f = 1.28f_\pi, \quad f_\pi = 93 \text{ MeV}, \quad (5)$$

with k^0, k'^0 the energies of the pseudoscalar mesons, and C_{ij} the coefficients given in Tables A.4.2 and A.4.3 of Ref. [11]. The scattering matrix is obtained via the Bethe-Salpeter equation in matrix form

$$T = [1 - VG]^{-1}V, \quad (6)$$

with G the meson-baryon loop function, regularized with a cutoff $q_{\max} = 830$ MeV, to get a good reproduction of the BESIII data [17,18].

Below, we show the details for the calculation of the $\pi\Xi^*$ and $\bar{K}\Sigma^*$ invariant mass distributions of the reactions $\Omega_c^0 \rightarrow \pi^+(\pi^0, \eta)\pi\Xi^*$ and $\Omega_c^0 \rightarrow \pi^+(\pi^0, \eta)\bar{K}\Sigma^*$.

B. The Ω_c^0 decay to $\pi^+(\pi^0, \eta)\pi\Xi^*$

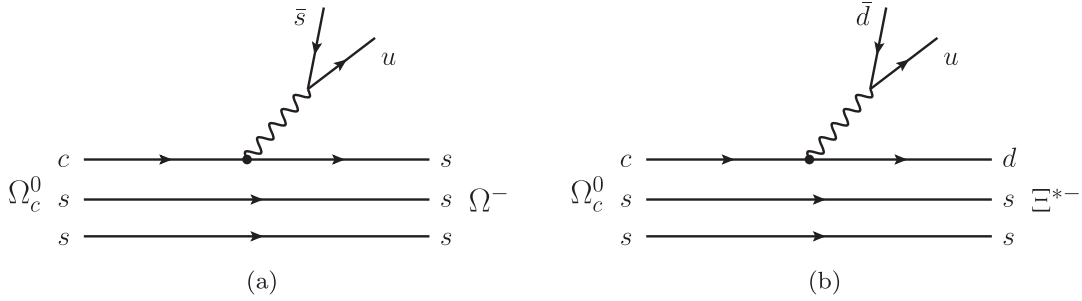
The process that we study is single Cabibbo suppressed. We consider the dominant external emission mechanism. At the quark level, we have two topologies that can lead to the desired final state depicted in Figs. 1(a) and 1(b). To obtain two mesons in the final state, we have to hadronize the $\bar{s}u$ and $\bar{d}u$ components. This is done by writing the matrix $q\bar{q}$ in terms of physical mesons, P ,

$$P = \begin{pmatrix} \frac{\pi^0}{\sqrt{2}} + \frac{\eta}{\sqrt{3}} & \pi^+ & K^+ \\ \pi^- & -\frac{\pi^0}{\sqrt{2}} + \frac{\eta}{\sqrt{3}} & K^0 \\ K^- & \bar{K}^0 & -\frac{\eta}{\sqrt{3}} \end{pmatrix}, \quad (7)$$

where the η - η' standard mixing of Ref. [25] is used and the η' , not playing a role in the energy region of relevance, is omitted. Then,

$$\begin{aligned}u\bar{s} &\rightarrow \sum_i u\bar{q}_i q_i \bar{s} = P_{1i}P_{i3} = (P^2)_{13} \\ &= \left(\frac{\pi^0}{\sqrt{2}} + \frac{\eta}{\sqrt{3}}\right)K^+ + \pi^+K^0 - \frac{1}{\sqrt{3}}K^+\eta.\end{aligned}\quad (8)$$

It might look like the ηK^+ component cancels, but this is not the case, as we see below, because the order matters:


 FIG. 1. The two topological structures with external emission that lead to Ω^- (a) and Ξ^{*-} (b) in the final state.

$$\begin{aligned}
 u\bar{d} &\rightarrow \sum_i u\bar{q}_i q_i \bar{d} = P_{1i} P_{i2} = (P^2)_{12} \\
 &= \left(\frac{\pi^0}{\sqrt{2}} + \frac{\eta}{\sqrt{3}} \right) \pi^+ + \pi^+ \left(-\frac{\pi^0}{\sqrt{2}} + \frac{\eta}{\sqrt{3}} \right) + K^+ \bar{K}^0. \quad (9)
 \end{aligned}$$

Once again, the $\pi^0\pi^+$ component does not cancel, but the $\eta\pi^+$ does, as we see below.

The coupling of W^+ to the meson-meson component has the structure of $\langle [P, \partial_\mu P] W^\mu T_- \rangle$, with T_- a matrix related to the Kobayashi-Maskawa elements [26,27]. The csW vertex is of the type $\gamma^\mu(1 - \gamma_5)$, and the resulting weak transition operator at the quark level is $(p_1 - p_2)_\mu \gamma^\mu(1 - \gamma_5)$ with p_1, p_2 the momenta of the first, second mesons. But we have to make a transition from a spin $1/2^+$ state (Ω_c^0) to a $3/2^+$ state Ω^- or Ξ^{*-} (1530), which requires a spin operator at the quark level, and we need then the term $(p_1 - p_2)^i \gamma^i \gamma_5 \rightarrow \sigma^i (p_1 - p_2)^i$. This operator at the macroscopic level between the Ω_c^0 and the Ω^-, Ξ^{*-} states has the type

$$\langle \Omega^-(\Xi^{*-}(1530)) | \vec{S}^+ \cdot (\vec{p}_1 - \vec{p}_2) | \Omega_c^0 \rangle, \quad (10)$$

where S^+ is the spin transition operator from spin $1/2$ to spin $3/2$, which has the property in Cartesian basis

$$\sum_M S_i |M\rangle \langle M | S_j^+ = \frac{2}{3} \delta_{ij} - \frac{i}{3} \epsilon_{ijk} \sigma_k. \quad (11)$$

From this perspective, we see that the ηK^+ and $-K^+\eta$ terms in Eq. (8) give the same contribution, and so do the $\pi^0\pi^+$ and $-\pi^+\pi^0$ of Eq. (9), while the terms $\eta\pi^+$ and $\pi^+\eta$ of Eq. (9) cancel.

The mechanisms of Figs. 1(a) and 1(b) share the same Cabibbo strength factor $\cos\theta_c \sin\theta_c$, but the matrix elements are different. Indeed, we have for the mechanism of Fig. 1(a)

$$\langle sss\chi_S | \vec{\sigma} \cdot (\vec{p}_1 - \vec{p}_2) \bar{c}s | css\chi_{MS} \rangle = \langle \chi_S | \vec{\sigma} \cdot (\vec{p}_1 - \vec{p}_2) | \chi_{MS} \rangle, \quad (12)$$

while for Fig. 1(b) we have

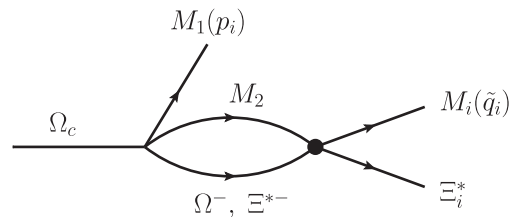
$$\begin{aligned}
 &\left\langle \frac{1}{\sqrt{3}} (dss + sds + ssd) \chi_S \left| \vec{\sigma} \cdot (\vec{p}_1 - \vec{p}_2) \bar{c}d \right| css\chi_{MS} \right\rangle \\
 &= \frac{1}{\sqrt{3}} \langle \chi_S | \vec{\sigma} \cdot (\vec{p}_1 - \vec{p}_2) | \chi_{MS} \rangle, \quad (13)
 \end{aligned}$$

where χ_S and χ_{MS} are the spin symmetric and mixed symmetric wave functions. Hence we see that the two matrix elements have the same spin structure, but the flavor structure gives an extra factor $\frac{1}{\sqrt{3}}$ for the mechanism of Fig. 1(b). Note that we take the $css\chi_{MS}$ structure for the Ω_c^0 state, singling out the c quark, following Refs. [28,29].

To generate the $\Xi(1820)$ resonance in the final state, we have to allow one of the mesons to interact with the Ω^- or Ξ^{*-} , and this leads to the picture of Fig. 2. The structure of Fig. 2 corresponds to an amplitude of the type

$$\begin{aligned}
 &\int_{|\vec{p}_2| < q_{\max}} \frac{d^3 p_2}{(2\pi)^3} \langle \Omega^- | \vec{S}^+ \cdot (\vec{p}_1 - \vec{p}_2) | \Omega_c^0 \rangle \\
 &\cdot \frac{1}{2\omega(p_2) E_B(p_2) M_{\text{inv}} - \omega(p_2) - E_B(p_2) + i\epsilon} \\
 &\cdot t_{M_2 B, M_i \Xi_i^*} (M_{\text{inv}}(M_i \Xi_i^*)), \quad (14)
 \end{aligned}$$

where $\omega(p_2) = \sqrt{\vec{p}_2^2 + m_{M_2}^2}$, $E_B(p_2) = \sqrt{\vec{p}_2^2 + m_B^2}$, with M_2, B the intermediate meson, baryon states in the loop, and $t_{M_2 B, M_i \Xi_i^*}$ the transition scattering matrix from $M_2 B$ to $M_i \Xi_i^*$. Since $t_{M_2 B, M_i \Xi_i^*}$ is constructed with the S -wave potential of Eq. (5), the term with \vec{p}_2 in Eq. (14) does not contribute, hence, only the $\vec{S}^+ \cdot \vec{p}_1$, corresponding to


 FIG. 2. Final state interaction of a meson with the baryon of the decuplet $3/2^+$. The dot indicates the transition matrix element from $M_2\Omega^-(\Xi^{*-})$ to a final $M_i\Xi_i^*$ state.

the external meson in the weak vertex, contributes. Then the spin matrix element of Eq. (14) factorizes out of the integral and so does $t_{M_2 B, M_i \Xi_i^*}$. We should recall that in the mechanism of Fig. 2 the dynamics of the weak decay selected the channels $M_2 \Omega^-$ and $M_2 \Xi^{*-}$ in the loop, and we chose the final states $M_i \Xi_i^*$ which are open for decay of the $\Xi(1820)$ resonances. However, in the transition matrices $t_{M_2 \Omega^-, M_i \Xi_i^*}$ and $t_{M_2 \Xi^{*-}, M_i \Xi_i^*}$ we have the contribution of all the channels, via the Bethe-Salpeter equation in coupled channels, Eq. (6), used to generate these amplitudes.

All this said, we have six possible reactions written below, where the first meson corresponds to the external one of the weak vertex and the second one to the final state. The corresponding amplitudes are written for each case. First we look at the terms originating from Fig. 1(a), with an Ω^- in the intermediate state,

$$(1) \quad \Omega_c^0 \rightarrow \pi^+ \pi^0 \Xi^{*-}$$

$$\begin{aligned} t_1 &= C \langle \Omega^- | \vec{S}^+ \cdot \vec{p}_{\pi^+} | \Omega_c^0 \rangle t'_1, \\ t'_1 &= G_{K^0 \Omega^-} (M_{\text{inv}}(\pi^0 \Xi^{*-})) \cdot t_{K^0 \Omega^-, \pi^0 \Xi^{*-}} (M_{\text{inv}}(\pi^0 \Xi^{*-})); \end{aligned} \quad (15)$$

$$(2) \quad \Omega_c^0 \rightarrow \pi^+ \pi^- \Xi^{*0}$$

$$\begin{aligned} t_2 &= C \langle \Omega^- | \vec{S}^+ \cdot \vec{p}_{\pi^+} | \Omega_c^0 \rangle t'_2, \\ t'_2 &= G_{K^0 \Omega^-} (M_{\text{inv}}(\pi^- \Xi^{*0})) \cdot t_{K^0 \Omega^-, \pi^- \Xi^{*0}} (M_{\text{inv}}(\pi^- \Xi^{*0})); \end{aligned} \quad (16)$$

$$(3) \quad \Omega_c^0 \rightarrow \pi^0 \pi^+ \Xi^{*-}$$

$$\begin{aligned} t_3 &= C \langle \Omega^- | \vec{S}^+ \cdot \vec{p}_{\pi^0} | \Omega_c^0 \rangle t'_3, \\ t'_3 &= \frac{1}{\sqrt{2}} G_{K^+ \Omega^-} (M_{\text{inv}}(\pi^+ \Xi^{*-})) \\ &\quad \cdot t_{K^+ \Omega^-, \pi^+ \Xi^{*-}} (M_{\text{inv}}(\pi^+ \Xi^{*-})); \end{aligned} \quad (17)$$

$$(4) \quad \Omega_c^0 \rightarrow \pi^0 \pi^0 \Xi^{*0}$$

$$\begin{aligned} t_4 &= C \langle \Omega^- | \vec{S}^+ \cdot \vec{p}_{\pi^0} | \Omega_c^0 \rangle t'_4, \\ t'_4 &= \frac{1}{\sqrt{2}} G_{K^+ \Omega^-} (M_{\text{inv}}(\pi^0 \Xi^{*0})) \\ &\quad \cdot t_{K^+ \Omega^-, \pi^0 \Xi^{*0}} (M_{\text{inv}}(\pi^0 \Xi^{*0})); \end{aligned} \quad (18)$$

$$(5) \quad \Omega_c^0 \rightarrow \eta \pi^+ \Xi^{*-}$$

$$\begin{aligned} t_5 &= C \langle \Omega^- | \vec{S}^+ \cdot \vec{p}_{\eta} | \Omega_c^0 \rangle t'_5, \\ t'_5 &= \frac{2}{\sqrt{3}} G_{K^+ \Omega^-} (M_{\text{inv}}(\pi^+ \Xi^{*-})) \\ &\quad \cdot t_{K^+ \Omega^-, \pi^+ \Xi^{*-}} (M_{\text{inv}}(\pi^+ \Xi^{*-})); \end{aligned} \quad (19)$$

$$(6) \quad \Omega_c^0 \rightarrow \eta \pi^0 \Xi^{*0}$$

$$\begin{aligned} t_6 &= C \langle \Omega^- | \vec{S}^+ \cdot \vec{p}_{\eta} | \Omega_c^0 \rangle t'_6, \\ t'_6 &= \frac{2}{\sqrt{3}} G_{K^+ \Omega^-} (M_{\text{inv}}(\pi^0 \Xi^{*0})) \\ &\quad \cdot t_{K^+ \Omega^-, \pi^0 \Xi^{*0}} (M_{\text{inv}}(\pi^0 \Xi^{*0})); \end{aligned} \quad (20)$$

where C is a normalization constant, common to all terms.

Next we look at the amplitudes stemming from Fig. 1(b), leading to a Ξ^{*-} in the intermediate state. We have

$$(7) \quad \Omega_c^0 \rightarrow \pi^+ \pi^0 \Xi^{*-}$$

$$\begin{aligned} t_7 &= C \langle \Xi^{*-} | \vec{S}^+ \cdot \vec{p}_{\pi^+} | \Omega_c^0 \rangle t'_7, \\ t'_7 &= -\sqrt{\frac{2}{3}} [1 + G_{\pi^0 \Xi^{*-}} (M_{\text{inv}}(\pi^0 \Xi^{*-})) \\ &\quad \cdot t_{\pi^0 \Xi^{*-}, \pi^0 \Xi^{*-}} (M_{\text{inv}}(\pi^0 \Xi^{*-}))]; \end{aligned} \quad (21)$$

$$(8) \quad \Omega_c^0 \rightarrow \pi^+ \pi^- \Xi^{*0}$$

$$\begin{aligned} t_8 &= C \langle \Xi^{*-} | \vec{S}^+ \cdot \vec{p}_{\pi^+} | \Omega_c^0 \rangle t'_8, \\ t'_8 &= -\sqrt{\frac{2}{3}} G_{\pi^0 \Xi^{*-}} (M_{\text{inv}}(\pi^- \Xi^{*0})) \\ &\quad \cdot t_{\pi^0 \Xi^{*-}, \pi^- \Xi^{*0}} (M_{\text{inv}}(\pi^- \Xi^{*0})); \end{aligned} \quad (22)$$

$$(9) \quad \Omega_c^0 \rightarrow \pi^0 \pi^+ \Xi^{*-}$$

$$\begin{aligned} t_9 &= C \langle \Xi^{*-} | \vec{S}^+ \cdot \vec{p}_{\pi^0} | \Omega_c^0 \rangle t'_9, \\ t'_9 &= \sqrt{\frac{2}{3}} [1 + G_{\pi^+ \Xi^{*-}} (M_{\text{inv}}(\pi^+ \Xi^{*-})) \\ &\quad \cdot t_{\pi^+ \Xi^{*-}, \pi^+ \Xi^{*-}} (M_{\text{inv}}(\pi^+ \Xi^{*-}))]; \end{aligned} \quad (23)$$

$$(10) \quad \Omega_c^0 \rightarrow \pi^0 \pi^0 \Xi^{*0}$$

$$\begin{aligned} t_{10} &= C \langle \Xi^{*-} | \vec{S}^+ \cdot \vec{p}_{\pi^0} | \Omega_c^0 \rangle t'_{10}, \\ t'_{10} &= \sqrt{\frac{2}{3}} G_{\pi^+ \Xi^{*-}} (M_{\text{inv}}(\pi^0 \Xi^{*0})) \\ &\quad \cdot t_{\pi^+ \Xi^{*-}, \pi^0 \Xi^{*0}} (M_{\text{inv}}(\pi^0 \Xi^{*0})). \end{aligned} \quad (24)$$

The cases (7)–(10) in Eqs. (21)–(24) correspond to the same final state than for the cases (1)–(4) and have to be added coherently. In the amplitudes of Eqs. (21) and (23) for cases (7) and (9), we have also added the tree level contribution. For these terms the contribution of \vec{p}_2 in $\vec{S}^+ \cdot (\vec{p}_1 - \vec{p}_2)$ should also be kept, but in the region of invariant masses of $M_2 B$ that we are interested, it is easy to see that $|\vec{p}_1|$ is more than an order of magnitude bigger than $|\vec{p}_2|$, and we disregard p_2 , which makes the formalism more compact.

Summing coherently the amplitudes for the mechanisms of Figs. 1(a) and 1(b), we arrive at the final formula for the different reactions

$$t_i = C\langle \Xi^*(3/2^+) | \vec{S}^+ \cdot \vec{p}_i | \Omega_c^0 \rangle \tilde{t}_i, \quad (25)$$

with

$$\begin{aligned} \tilde{t}_1 &= t'_1 + t'_7, & \tilde{t}_2 &= t'_2 + t'_8, \\ \tilde{t}_3 &= t'_3 + t'_9, & \tilde{t}_4 &= t'_4 + t'_{10}, \\ \tilde{t}_5 &= t'_5, & \tilde{t}_6 &= t'_6. \end{aligned} \quad (26)$$

In Eq. (25), the baryon $\Xi^*(3/2^+)$ should be the baryon B of the loop, but since the $t_{M_2 B, M_i \Xi_i^*}$ is spin independent, the spin of the intermediate B baryon is transferred to the final Ξ^* state, resulting in the formula of Eq. (25).

Finally, once the t_i matrices have been constructed, the mass distribution for the final $M_i \Xi_i^*$ pair is given by

$$\frac{d\Gamma_i}{dM_{\text{inv}}(M_i \Xi_i^*)} = \frac{1}{(2\pi)^3} \frac{1}{4M_{\Omega_c}^2} p_i \tilde{q}_i \sum_{\vec{m}} \sum |t_i|^2 \quad (i = 1 \sim 6), \quad (27)$$

where p_i is the momentum of the external meson in the weak vertex in the Ω_c^0 rest frame and \tilde{q}_i is the momentum of the meson M_i of the final $M_i \Xi_i^*$ pair in the rest frame of that pair. The magnitude $\sum_{\vec{m}} |t_i|^2$, taking into account Eq. (11), is then given by

$$\sum_{\vec{m}} \sum |t_i|^2 = C^2 \frac{2}{3} \vec{p}_i^2 |\tilde{t}_i|^2. \quad (28)$$

We take $C^2 = 1$ in our calculations.

C. The Ω_c^0 decay to $\pi^+(\pi^0, \eta)\bar{K}\Sigma^*$

The choice of the final $\pi\Xi^*$ states in the former subsection is motivated because the threshold mass of this system is 1670 MeV, far below the 1820 and 1875 MeV of the two $\Xi(1820)$ resonances. Hence, the decay of the $\Xi(1820)$ states in the $\pi\Xi^*$ channels is guaranteed, and we could observe the effect of the two resonances. The other possible decay channel is $\bar{K}\Sigma^*$, but the threshold of this channel is 1878 MeV, which technically would allow the observation of the $\Xi(1875)$ but not the lower mass state $\Xi(1820)$. However, due to the width of the Σ^* , $\Gamma_{\Sigma^*} = 37.2$ MeV, we can go below that threshold and still see the effect of the lower $\Xi(1820)$ state. Yet, we can anticipate that the contribution of this state will be much suppressed, and hence the effect of the high mass $\Xi(1875)$ state will be relatively magnified. In this case, the information obtained from the decay of Ω_c^0 to the $M_1 \Xi(1820)$ with the two $\Xi(1820)$ resonances decaying into $\bar{K}\Sigma^*$ should bring very

valuable complementary information concerning the existence of these two states.

In view of that we evaluate here the $\bar{K}\Sigma^*$ mass distributions for the reactions $\Omega_c^0 \rightarrow \pi^+ \bar{K}^0 \Sigma^{*-}$, $\pi^+ K^- \Sigma^{*0}$, $\pi^0 \bar{K}^0 \Sigma^{*0}$, $\pi^0 K^- \Sigma^{*+}$, $\eta \bar{K}^0 \Sigma^{*0}$, and $\eta K^- \Sigma^{*+}$. The formalism is similar to the one described in Sec. II B. The $t_i^{(K)}$ ($i = 1, 2, \dots, 10$) amplitudes are formally the same with the substitution

$$\begin{aligned} t_{K\Omega^-, \pi_i \Xi_i^*} &\rightarrow t_{K\Omega^-, \bar{K}_j \Sigma_j^*}, \\ t_{\pi \Xi^*, \pi_i \Xi_i^*} &\rightarrow t_{\pi \Xi^*, \bar{K}_j \Sigma_j^*}, \end{aligned} \quad (29)$$

but in $t_7^{(K)}$ and $t_9^{(K)}$ there is no tree level [term 1 in Eqs. (21) and (23)]. More concretely the changes of the $\bar{K}_j \Sigma_j^*$ final states, in t_1, \dots, t_{10} , are

$$\begin{aligned} t_1^{(K)} &: t_{K^0 \Omega^-, \pi^0 \Xi^{*-}} \rightarrow t_{K^0 \Omega^-, \bar{K}^0 \Sigma^{*-}}, \\ t_2^{(K)} &: t_{K^0 \Omega^-, \pi^- \Xi^{*0}} \rightarrow t_{K^0 \Omega^-, K^- \Sigma^{*0}}, \\ t_3^{(K)} &: t_{K^+ \Omega^-, \pi^+ \Xi^{*-}} \rightarrow t_{K^+ \Omega^-, \bar{K}^0 \Sigma^{*0}}, \\ t_4^{(K)} &: t_{K^+ \Omega^-, \pi^0 \Xi^{*0}} \rightarrow t_{K^+ \Omega^-, K^- \Sigma^{*+}}, \\ t_5^{(K)} &: t_{K^+ \Omega^-, \pi^+ \Xi^{*-}} \rightarrow t_{K^+ \Omega^-, \bar{K}^0 \Sigma^{*0}}, \\ t_6^{(K)} &: t_{K^+ \Omega^-, \pi^0 \Xi^{*0}} \rightarrow t_{K^+ \Omega^-, K^- \Sigma^{*+}}, \\ t_7^{(K)} &: t_{\pi^0 \Xi^{*-}, \pi^0 \Xi^{*-}} \rightarrow t_{\pi^0 \Xi^{*-}, \bar{K}^0 \Sigma^{*-}}, \\ t_8^{(K)} &: t_{\pi^0 \Xi^{*-}, \pi^- \Xi^{*0}} \rightarrow t_{\pi^0 \Xi^{*-}, K^- \Sigma^{*0}}, \\ t_9^{(K)} &: t_{\pi^+ \Xi^{*-}, \pi^+ \Xi^{*-}} \rightarrow t_{\pi^+ \Xi^{*-}, \bar{K}^0 \Sigma^{*0}}, \\ t_{10}^{(K)} &: t_{\pi^+ \Xi^{*-}, \pi^0 \Xi^{*0}} \rightarrow t_{\pi^+ \Xi^{*-}, K^- \Sigma^{*+}}. \end{aligned} \quad (30)$$

The rest of the equations follow as in the former subsection, but since the $\bar{K}\Sigma^*$ threshold is so close to the energies of the two $\Xi(1820)$ states, we take into account explicitly the mass distribution of the Σ^* through its spectral function

$$\begin{aligned} S_{\Sigma^*}(M_{\text{inv}}(\Sigma^*)) &= -\frac{1}{\pi} \text{Im} \frac{1}{M_{\text{inv}}(\Sigma^*) - M_{\Sigma^*} + i\Gamma_{\Sigma^*}(M_{\text{inv}}(\Sigma^*))/2}, \end{aligned} \quad (31)$$

where

$$\Gamma_{\Sigma^*}(M_{\text{inv}}(\Sigma^*)) = \Gamma_{\Sigma^*, \text{on}} \frac{M_{\Sigma^*}}{M_{\text{inv}}(\Sigma^*)} \left(\frac{\tilde{p}_\pi}{\tilde{p}_{\pi, \text{on}}} \right)^3, \quad (32)$$

with $M_{\Sigma^*} = 1384.6$ MeV and $\Gamma_{\Sigma^*, \text{on}} = 37.2$ MeV being the average mass and width of Σ^* , and we consider \tilde{p}_π the momentum of the π in the decay of Σ^* with mass $M_{\text{inv}}(\Sigma^*)$ to $\pi\Lambda$ (the decay mode accounting by 87% of the Σ^* decay width), and $\tilde{p}_{\pi, \text{on}}$ the same magnitude for the nominal mass of the Σ^* . We consider that the Σ^* will be measured in the

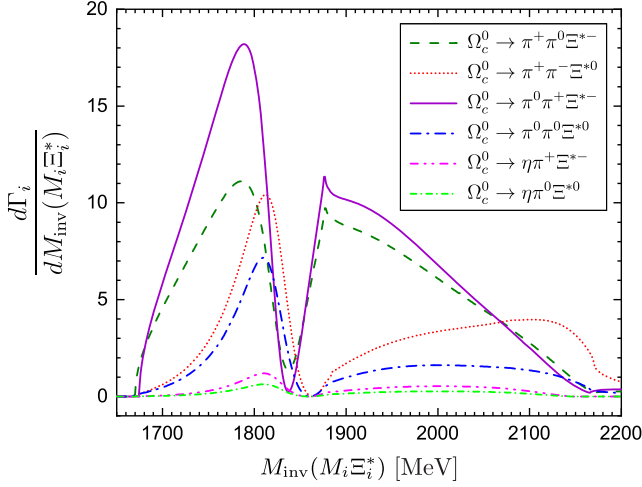


FIG. 3. $M_{\text{inv}}(M_i \Xi_i^*)$ invariant mass distributions for the $\Omega_c^0 \rightarrow M_1 M_i \Xi_i^*$ decays.

$\pi\Lambda$ decay mode and then Eq. (27) will be substituted by

$$\begin{aligned} & \frac{d\Gamma_i}{dM_{\text{inv}}(\bar{K}\Sigma^*)dM_{\text{inv}}(\Sigma^*)} \\ &= \frac{\Gamma_{\Sigma^* \rightarrow \pi\Lambda}}{\Gamma_{\Sigma^*, \text{on}}} \cdot S_{\Sigma^*}(M_{\text{inv}}(\Sigma^*)) \\ & \times \frac{1}{(2\pi)^3} \frac{1}{4M_{\Omega_c}^2} p_i \tilde{q}_i \sum \sum |t_i^{(K)}|^2, \end{aligned} \quad (33)$$

where

$$\begin{aligned} p_i &= \frac{\lambda^{1/2}(M_{\Omega_c}^2, m_{M_1}^2, M_{\text{inv}}^2(\bar{K}\Sigma^*))}{2M_{\Omega_c}}, \\ \tilde{q}_i &= \frac{\lambda^{1/2}(M_{\text{inv}}^2(\bar{K}\Sigma^*), m_K^2, M_{\text{inv}}^2(\Sigma^*))}{2M_{\text{inv}}(\bar{K}\Sigma^*)}, \end{aligned} \quad (34)$$

with $\lambda(x, y, z) = x^2 + y^2 + z^2 - 2xy - 2xz - 2yz$ the Källén function, and we will integrate over $dM_{\text{inv}}(\Sigma^*)$ to obtain $d\Gamma_i/dM_{\text{inv}}(\bar{K}\Sigma^*)$.

III. RESULTS

First, we show the results for the $\Omega_c^0 \rightarrow \pi^+(\pi^0, \eta)\pi\Xi^*$ reactions.

In Fig. 3 we show the mass distribution of the final pair for the six reactions that we have studied. As we can see, the shapes of the $M_{\text{inv}}(M_i \Xi_i^*)$ distributions for the reactions are different from each other, but they share something in common: there is a dip in the mass distribution around 1850 MeV, which is even a zero in all but two of the distributions. This is due to the destructive interference of the two resonances, a reminiscence of what happens with the $f_0(500)$ and $f_0(980)$ resonances in S -wave $\pi\pi$ scattering, where the $f_0(980)$ shows up in the cross section as a dip, not as a peak. This feature does not preclude that the

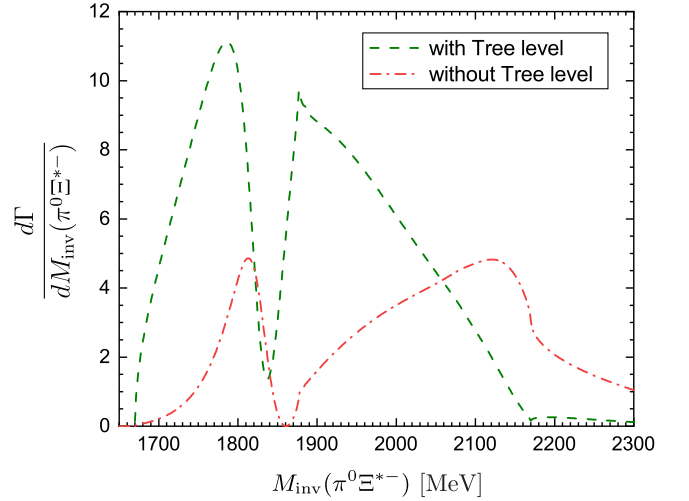


FIG. 4. $M_{\text{inv}}(\pi^0 \Xi^{*-})$ invariant mass distribution for the $\Omega_c^0 \rightarrow \pi^+ \pi^0 \Xi^{*-}$ decay.

$f_0(980)$ can show up as a peak in many other reactions [30], which means that the two $\Xi(1820)$ states can show up also in a different way, as is the case of the $\psi(3686) \rightarrow K^- \Lambda \Xi^+$ BESIII reaction [17]. The two reactions where the mass distribution does not go to zero are those where the tree level is present.

The mass distributions show two peaks, and it is important not to misidentify them. They do not correspond to the two resonances that we are discussing. They come from the interference of the two resonance contributions. It is important to notice that the two reactions that contain the tree level contribution, $\Omega_c^0 \rightarrow \pi^0 \pi^+ \Xi^{*-}$ and $\Omega_c^0 \rightarrow \pi^+ \pi^0 \Xi^{*-}$, have the two peaks more pronounced, and the width of the peaks also do not reflect the widths of the states that we have. To clarify what happens we show in Fig. 4 the mass distribution for the $\Omega_c^0 \rightarrow \pi^+ \pi^0 \Xi^{*-}$ reaction removing the tree level contribution. The peak to the left certainly reflects our first state at 1824 MeV, with an apparent width of around 40 MeV, even smaller than the one we get from the pole position, 62 MeV, due to the interference with the second resonance. The shape of the second resonance, with a width of 260 MeV from the pole position, cannot be distinguished due again to the destructive interference with the first peak, but one can guess that it is a broad resonance; otherwise, one could still see a sharper structure than the one we obtain around 1900–2000 MeV. It is interesting to see that around 2150 MeV there is another peak. This corresponds to a third resonance obtained in Ref. [18] and also Ref. [11] around that energy.

After this discussion it becomes clear that the reactions free of tree level contribution show more clearly the resonance structure. Coming back to Fig. 3, these are the reactions: $\Omega_c^0 \rightarrow \pi^+ \pi^- \Xi^{*0}$, $\Omega_c^0 \rightarrow \pi^0 \pi^0 \Xi^{*0}$, $\Omega_c^0 \rightarrow \eta \pi^+ \Xi^{*-}$, and $\Omega_c^0 \rightarrow \eta \pi^0 \Xi^{*0}$. The first peak corresponding to the lower $\Xi(1820)$ resonance is clearly seen, and the interference

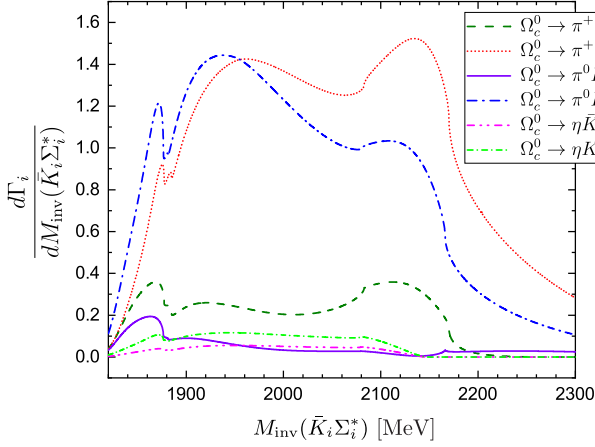


FIG. 5. $M_{\text{inv}}(\bar{K}_i \Sigma_i^*)$ invariant mass distributions for the $\Omega_c^0 \rightarrow M_1 \bar{K}_i \Sigma_i^*$ decays.

pattern is very similar in all the reactions. The peak corresponding to a third resonance around 2150 MeV is better seen in the $\Omega_c^0 \rightarrow \pi^+ \pi^- \Xi^{*0}$ reaction.

One word of caution should be said here. If we have the $\Omega_c^0 \rightarrow \pi^0 \pi^0 \Xi^{*0}$ reaction, we should have symmetrized our amplitude with respect to the two π^0 identical states. We have not done it because the kinematics of these two π^0 are very different and one can clearly distinguish them. One can see that the external π^0 coming from the weak vertex has a momentum around 770 MeV while the π^0 from the $\pi^0 \Xi^{*0}$ resonance state has about 50 MeV. They are easily distinguished experimentally as shown in Ref. [31]. This argument also holds to distinguish the two pions in other reactions into the one coming from the weak vertex and the one belonging to the resonance.

We show next the results of the mass distributions with $\bar{K}\Sigma^*$ in the final state. The results obtained are shown in Figs. 5 and 6.

In Fig. 5, we observe that the $\Omega_c \rightarrow \pi^0 K^- \Sigma^{*+}$ and $\Omega_c \rightarrow \pi^+ K^- \Sigma^{*0}$ decays have the biggest strength, followed by the $\Omega_c \rightarrow \pi^+ \bar{K}^0 \Sigma^{*-}$. The structure of the line shape is very instructive. The consideration of the width of the Σ^* allows us to go below the nominal $\bar{K}\Sigma$ threshold and still see a contribution from the lower mass $\Xi(1820)$ state. Yet, unlike in the case of the $\psi(3686)$ decay in the BESIII experiment [17], where the contribution of the lower mass state was dominant, this is not the case here, and we have a large contribution of the second state around 1900 MeV, mostly visible in the two reactions with the largest strength. It is interesting to note that we also observe a peak around 2110 MeV that corresponds to another Ξ resonance obtained in Ref. [11]. Some indication of the existence of this resonance was already observed in the data of the BESIII experiment [17].

Figure 6 is a blowup of the results for the reactions with smaller strengths. In Fig. 6, we have similar features as in Fig. 5, but the strength is smaller. The $\Omega_c \rightarrow$

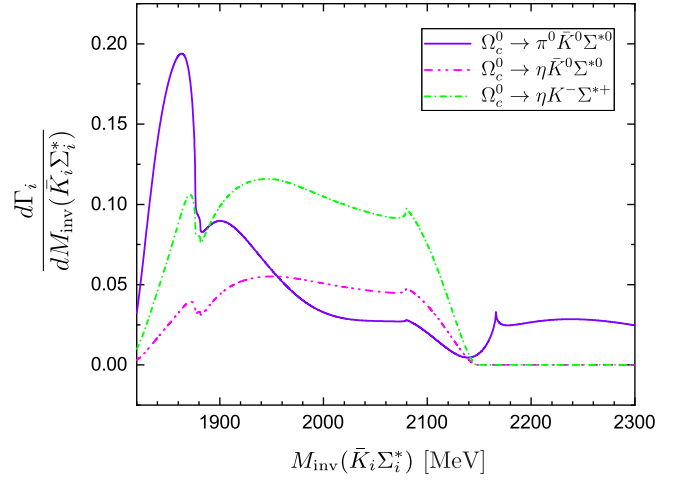


FIG. 6. $M_{\text{inv}}(\bar{K}_i \Sigma_i^*)$ invariant mass distributions for the $\Omega_c^0 \rightarrow M_1 \bar{K}_i \Sigma_i^*$ decays.

$\eta \bar{K}^0 \Sigma^{*0}, \eta K^- \Sigma^{*+}$ decays have a mass distribution similar to that obtained for the other channels but with smaller strengths. The $\Omega_c \rightarrow \pi^0 \bar{K}^0 \Sigma^{*0}$ decay has a peculiar shape because one finds a destructive interference between the $\Xi(1875)$ and the Ξ resonances at 2100 MeV, resulting in a dip, rather than a peak at 2100–2150 MeV. It is also worth noting that due to this interference, the contribution of the lower mass $\Xi(1820)$ state is now stressed, and a clean peak corresponding to this resonance shows up, with bigger strength than that of the higher mass state.

All these features tell us that the measurement of these decays and their mass distributions will shed much light on the existence of the two $\Xi(1820)$ resonances and the additional one around 2100–2150 MeV.

IV. CONCLUSIONS

In this work we have studied several reactions coming from the single Cabibbo suppressed weak decay of the Ω_c^0 state into two pseudoscalars and a Ξ^* state. One of the pseudoscalars interacts with the Ξ^* state to produce two resonances around 1820 MeV that were predicted in Ref. [11] and reconfirmed in Ref. [18]. These resonances played an important role describing the peak seen in the $K^- \Lambda$ mass distribution in the $\psi(3686)$ decay to $K^- \Lambda \bar{\Xi}^{*+}$ of the BESIII experiment [17].

In this work we study six reactions: $\Omega_c^0 \rightarrow \pi^+ \pi^0 \Xi^{*-}$, $\Omega_c^0 \rightarrow \pi^+ \pi^- \Xi^{*0}$, $\Omega_c^0 \rightarrow \pi^0 \pi^+ \Xi^{*-}$, $\Omega_c^0 \rightarrow \pi^0 \pi^0 \Xi^{*0}$, $\Omega_c^0 \rightarrow \eta \pi^+ \Xi^{*-}$, and $\Omega_c^0 \rightarrow \eta \pi^0 \Xi^{*0}$, where the first meson is produced at the weak vertex and the second meson comes from the decay of the resonances. We obtained mass distribution for the final pair which differed from each other in the different reactions. In particular, the shapes of the $\Omega_c^0 \rightarrow \pi^+ \pi^0 \Xi^{*-}$ and $\Omega_c^0 \rightarrow \pi^0 \pi^+ \Xi^{*-}$ were very different from the other ones, and this was traced back to

the contribution of the tree level mechanism to the reaction. The other four reactions did not have tree level contribution and required rescattering of meson-baryon where the resonances are produced. The shapes of these four reactions resembled each other and had as a distinct feature, very different from the one observed in the $\psi(3686)$ decay to $K^-\Lambda\bar{\Xi}^{*+}$, which is a dip of the mass distribution around 1850 MeV, that was due to a destructive interference between the two $\Xi(1820)$ states. This pattern reminds one of the same thing happening in the S -wave $\pi\pi$ cross section around 980 MeV, where a dip is also observed as a consequence of the destructive interference between the $f_0(500)$ and the $f_0(980)$ resonances.

We have also studied six more decay modes: $\Omega_c^0 \rightarrow \pi^+\bar{K}^0\Sigma^{*-}$, $\pi^+K^-\Sigma^{*0}$, $\pi^0\bar{K}^0\Sigma^{*0}$, $\pi^0K^-\Sigma^{*+}$, $\eta\bar{K}^0\Sigma^{*0}$, $\eta K^-\Sigma^{*+}$; and from them we found very different mass distributions from the former ones. The larger mass of $\bar{K}\Sigma^*$ versus $\pi\Xi^*$ reduces the phase space for the decay of the lower mass $\Xi(1820)$ resonance and thus magnifies the relative importance of the $\Xi(1875)$. In addition, in several cases one observes a clear peak for the excitation of another Ξ resonance around 2100–2150 MeV already hinted in the BESIII experiment [17], while in the $\Omega_c^0 \rightarrow \pi^0\bar{K}^0\Sigma^{*0}$ it appears as a dip, as a consequence of a destructive interference. It is clear that the observation of all these reactions should give us much information on the two $\Xi(1820)$ states and in addition the new Ξ resonance around 2100–2150 MeV.

At present many Cabibbo favored Ω_c^0 decays into strangeness $S = -3$ states have been reported in the

PDG [3], but updates of Belle and LHCb will open the door to the observation of single Cabibbo decay modes, as the one reported here. We are looking forward to these updates, encouraging the performance of the suggested experiments which will shed light on the existence of two close by $\Xi(1820)$ states, and related to it, on the nature of such states.

ACKNOWLEDGMENTS

R. M. acknowledges support from the Programa de apoyo a personas con talento Plan GenT program with Grant No. CIDEAGENT/2019/015, the Spanish Ministerio de Economía y Competitividad, and European Union (NextGenerationEU/PRTR) by Grant No. CNS2022-136146. This work is partly supported by the National Natural Science Foundation of China (NSFC) under Grants No. 12365019 and No. 11975083, and by the Central Government Guidance Funds for Local Scientific and Technological Development, China (Grant No. Guike ZY22096024). This work is also partly supported by the Spanish Ministerio de Economía y Competitividad (MINECO) and European FEDER funds under Contracts No. FIS2017-84038-C2-1-P B and No. PID2020-112777 GB-I00, and by Generalitat Valenciana under Contract No. PROMETEO/2020/023. This project has received funding from the European Union Horizon 2020 research and innovation programme under the program H2020-INFRAIA-2018-1, Grant Agreement No. 824093 of the STRONG-2020 project.

-
- [1] J. A. Oller and U. G. Meissner, *Phys. Lett. B* **500**, 263 (2001).
 - [2] D. Jido, J. A. Oller, E. Oset, A. Ramos, and U. G. Meissner, *Nucl. Phys. A* **725**, 181 (2003).
 - [3] R. L. Workman *et al.* (Particle Data Group), *Prog. Theor. Exp. Phys.* **2022**, 083C01 (2022).
 - [4] P. A. Zyla *et al.* (Particle Data Group), *Prog. Theor. Exp. Phys.* **2020**, 083C01 (2020).
 - [5] T. Hyodo and U.-G. Meißner, Pole Structure of the $\Lambda(1405)$ region, Review paper in the PDG [3].
 - [6] L. Roca, E. Oset, and J. Singh, *Phys. Rev. D* **72**, 014002 (2005).
 - [7] L. S. Geng, E. Oset, L. Roca, and J. A. Oller, *Phys. Rev. D* **75**, 014017 (2007).
 - [8] M. Albaladejo, P. Fernandez-Soler, F.-K. Guo, and J. Nieves, *Phys. Lett. B* **767**, 465 (2017).
 - [9] D. Gamermann, E. Oset, D. Strottman, and M. J. Vicente Vacas, *Phys. Rev. D* **76**, 074016 (2007).
 - [10] E. E. Kolomeitsev and M. F. M. Lutz, *Phys. Lett. B* **585**, 243 (2004).
 - [11] S. Sarkar, E. Oset, and M. J. Vicente Vacas, *Nucl. Phys. A* **750**, 294 (2005); **A780**, 90(E) (2006).
 - [12] B. Aubert *et al.* (BABAR Collaboration), *Phys. Rev. Lett.* **95**, 142001 (2005).
 - [13] B. Aubert *et al.* (BABAR Collaboration), *Phys. Rev. Lett.* **98**, 212001 (2007).
 - [14] M. Ablikim *et al.* (BESIII Collaboration), *Phys. Rev. D* **102**, 031101 (2020).
 - [15] J.-M. Xie, J.-X. Lu, L.-S. Geng, and B.-S. Zou, *Phys. Rev. D* **108**, L111502 (2023).
 - [16] U.-G. Meißner, *Symmetry* **12**, 981 (2020).
 - [17] M. Ablikim *et al.* (BESIII Collaboration), *Phys. Rev. D* **109**, 072008 (2024).
 - [18] R. Molina, W.-H. Liang, C.-W. Xiao, Z.-F. Sun, and E. Oset, *arXiv:2309.03618*.
 - [19] J. R. Pelaez, *Phys. Rep.* **658**, 1 (2016).
 - [20] J. A. Oller and E. Oset, *Nucl. Phys. A* **629**, 739 (1998).
 - [21] M. Ablikim *et al.* (BESIII Collaboration), *Phys. Rev. D* **92**, 052003 (2015); **93**, 039906(E) (2016).
 - [22] D. W. Thomas, A. Engler, H. E. Fisk, and R. W. Kraemer, *Nucl. Phys. B* **56**, 15 (1973).
 - [23] S. Prakhov *et al.* (Crystall Ball Collaboration), *Phys. Rev. C* **70**, 034605 (2004).

- [24] V. K. Magas, E. Oset, and A. Ramos, *Phys. Rev. Lett.* **95**, 052301 (2005).
- [25] A. Bramon, A. Grau, and G. Pancheri, *Phys. Lett. B* **283**, 416 (1992).
- [26] J. Gasser and H. Leutwyler, *Ann. Phys. (N.Y.)* **158**, 142 (1984).
- [27] S. Scherer, *Adv. Nucl. Phys.* **27**, 277 (2003).
- [28] S. Capstick and N. Isgur, *Phys. Rev. D* **34**, 2809 (1986).
- [29] W. Roberts and M. Pervin, *Int. J. Mod. Phys. A* **23**, 2817 (2008).
- [30] J. A. Oller, E. Oset, and A. Ramos, *Prog. Part. Nucl. Phys.* **45**, 157 (2000).
- [31] R. Aaij *et al.* (LHCb Collaboration), *J. High Energy Phys.* **04** (2019) 063.